

Surface-plasmon-enhanced transmission through metallic film perforated with fractal-featured aperture array

Yong-Jun Bao, Bo Zhang, Zhe Wu, Jian-Wen Si, Mu Wang,^{a)} and Ru-Wen Peng
National Laboratory of Solid State Microstructures and Department of Physics, Nanjing University,
Nanjing 210093, China

Xiang Lu, Jun Shao, and Zhi-feng Li
National Laboratory for Infrared Physics, Shanghai Institute of Technical Physics,
Chinese Academy of Sciences, Shanghai 200083, China

Xi-Ping Hao and Nai-Ben Ming
National Laboratory of Solid State Microstructures and Department of Physics, Nanjing University,
Nanjing 210093, China

(Received 10 April 2007; accepted 30 May 2007; published online 21 June 2007)

A fractal-featured metallic thin film with Sierpinski Carpet pattern is fabricated on silicon wafer by microfabrication techniques. Transmission infrared spectroscopy indicates that there exists extraordinary high transmission at specific wavelengths, which can be ascribed to the effect of surface plasmon resonance, and are determined by hierarchy of apertures of different sizes in the fractal structure. This patterned film provides a unique system to achieve enhanced transmission simultaneously at different selected frequencies of electromagnetic wave. © 2007 American Institute of Physics. [DOI: 10.1063/1.2750528]

Surface plasmon polariton (SPP) is an electromagnetic wave propagating along a dielectric-metal interface and is associated with surface free electron oscillation.¹⁻³ The field components of SPP decay exponentially in the media on both sides of the interface. The intrinsic two-dimensional nature of SPP provides significant flexibility in engineering the miniaturization of optical system and high-density integration of optical circuits.⁴⁻¹¹ It is therefore interesting to investigate the properties of wave excitation and propagation in such a system. Up to now, intensive studies have been carried out in the resonant transmission of light through subwavelength apertures perforated on a metal film.¹²⁻¹⁷ According to classic electrodynamics, the transmission of a subwavelength aperture is proportional to the fourth power of the ratio of its diameter and light wavelength,¹⁸ which becomes extremely low. However, when a metal film is perforated with periodic array of subwavelength holes, the optical transmission is tremendously enhanced than that predicted by the diffraction theory. The enhancement depends on array geometry (aperture diameter and spatial periodicity), wavelength of light, angle of incidence, as well as the type of material with which the structured film is made. The enhancement is also affected by the concrete shape of the apertures.¹⁹⁻²² This is a rapidly developing research area, and a thorough understanding of these unusual effects depends on large number of elaborately designed experiments.

Recently, transmission through an array of apertures in Penrose-tiling pattern, which has local rotation symmetry only, has been reported.²³ For aperiodic structures, another well known example is the Sierpinski Carpet, which composes of self-similar, iteratively shrinking square apertures arranged in a hierarchy manner, and contains apertures of different sizes on different scales. The fractal surface may be used as a unit cell of frequency selective surface to achieve

multiband structures.²⁴⁻²⁶ The enhanced transmission of a periodic array of square apertures attributed to SPPs has also been reported.²⁷ However, it seems that SPP excitation from a Sierpinski Carpet has not been well studied before. It is interesting to identify how the geometric self-similarity influences the enhanced transmission mediated by SPP. With this purpose, we apply microfabrication techniques to an aluminum film on a silicon wafer and generate a patterned metallic structure with fractal feature. The extraordinary optical transmission of this sample is investigated, and its physical origins are discussed.

The metallic fractal structure was fabricated on a double-polished silicon wafer 500 μm in thickness. A thin film of aluminum (500 nm in thickness) was deposited on the silicon wafer. The Sierpinski-Carpet with four iterative generations was fabricated using standard electron beam lithography. The metallic structure viewed by field emission scanning electron microscopy is shown in Fig. 1(a), where four iterations of originally square apertures can be identified. Figure 1(b) demonstrates the detailed structure of the marked region in Fig. 1(a), where the edge of the smallest square aperture is 2.0 μm . The whole sample had a dimension of 9.82

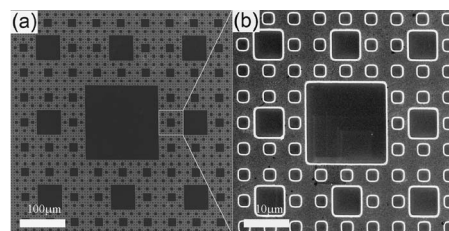


FIG. 1. (a) Scanning electron microscopy (SEM) micrograph of an aluminum thin film (500 nm thick) perforated with a fractal-featured aperture array with Sierpinski Carpet pattern on silicon wafer. Here the unit with four iterative generations is shown. The white bar represents 100 μm . (b) SEM micrograph of the marked region in (a). Two iterative generations can be identified. The bar represents 10 μm .

^{a)} Author to whom correspondence should be addressed; electronic mail: muwang@nju.edu.cn

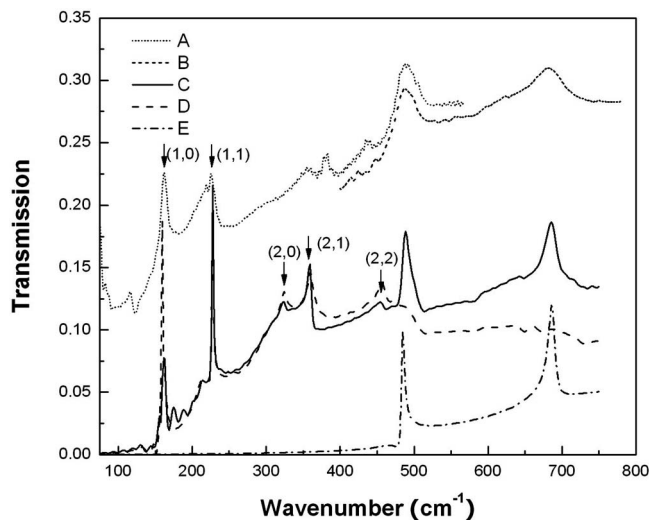


FIG. 2. Transmission spectra of the metallic Sierpinski Carpet structure. Curves A and B are the experimental spectra. A is the transmission spectrum measured with Bruker IFS66v/s, which has longer wavelength; B is measured with Bruker IFS66v/s, which covers shorter wavelength. The measurements are carried out on a sample with repeated unit as that shown in Fig. 1(a). C, D and E are the transmission spectra obtained by computer simulation. C is the calculated transmission spectrum of two iterations of Sierpinski-Carpet-like structure as shown in Fig. 3(a). D is the calculated transmission spectrum of the array of $6.0 \mu\text{m}$ square apertures, with the unit shown in Fig. 3(b). E is the calculated transmission spectrum from an array of $2 \mu\text{m}$ apertures as that shown in Fig. 3(c).

$\times 9.82 \text{ mm}^2$, and was composed of periodically duplicated Sierpinski Carpet pattern units of $486 \times 486 \mu\text{m}^2$ [each unit consisted of four iterative generations, as shown in Fig. 1(a)].

The transmission spectra were measured by vacuum infrared Fourier transform spectrometer (Bruker IFS66v/s and IFS66v, respectively) with normal incidence. The zero-order transmission spectra of the fractal structure were studied. A bare double-polished silicon wafer was used as a reference. In Fig. 2, plots A and B are the transmission spectra of the four iterative generations of metallic Sierpinski Carpet measured by two spectrometers at different wave bands. The peaks at 161.99 , 225.63 , 487.90 , and 682.68 cm^{-1} can be identified. In plots A and B, the peaks at 487.90 cm^{-1} coincide very well. The peaks can be grouped to two sets, 161.99 cm^{-1} , 225.63 cm^{-1} and 487.90 cm^{-1} , 682.68 cm^{-1} . The wave number of each pair of the corresponding peaks can be scaled by a factor of 3, which originates from the geometrical feature of Sierpinski Carpet pattern.

Numerical simulation was used to verify and analyze the experimental results. The simulation was performed with a commercial software (FULLWAVE 4.0) based on finite-difference-time-domain (FDTD) method. The Lorentz-Drude model proposed by Rakic et al. is used to describe the permittivity of aluminum.²⁸ This model takes both free electrons and bound electrons into account in considering the dispersion of metal. To simplify the simulation, both periodic boundary condition and perfect match layer condition are applied. Further, silicon substrate is simplified to a nonabsorbing medium with refractive index $n=3.4$, and the thickness is taken as infinite. Transmission spectra of three types of structured metallic films are simulated, which consist of $2.0 \mu\text{m}$ square aperture arrays, $6.0 \mu\text{m}$ square aperture arrays, and one iteration Sierpinski Carpet pattern with square apertures of 2.0 and $6.0 \mu\text{m}$. The morphologies of each unit

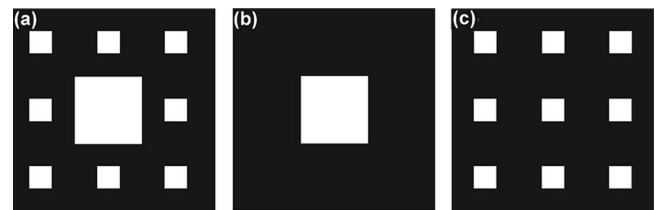


FIG. 3. Units used for computer simulation. (a) One iteration Sierpinski-Carpet-like pattern made of square apertures of 2.0 and $6.0 \mu\text{m}$ in size. The transmission spectrum of this structure is shown by curve C in Fig. 2. (b) $6.0 \mu\text{m}$ square aperture. The transmission spectrum of this structure is shown by curve D in Fig. 2. (c) Array of $2.0 \mu\text{m}$ square apertures. The transmission spectrum of this structure is shown by curve E in Fig. 2. In our computer calculation the basic units shown in (a)–(c) are all arranged in simple square lattice.

are shown in Fig. 3, and the units are arranged in simple square lattice for each scenario. As shown in Fig. 2, plot C corresponds to the resonance of one iteration Sierpinski-Carpet-like aperture array; plot D corresponds to the resonance of $6.0 \mu\text{m}$ square aperture array; and plot E corresponds to the resonance of $2.0 \mu\text{m}$ square aperture array. Immediately one may find that plot C coincides with the experimental data (plots A and B) at the four peaks mentioned in the last paragraph. We also compare the FDTD simulation results of plots C, D, and E. Plot C reproduces the salient features of the experimental spectra. However, the detailed shape of the calculated spectra does not agree quite well with the experimental data, which may be due to the fact that only one iterative generation of Sierpinski Carpet has been considered in simulation for the sake of limited calculation capability. The corresponding peaks as that shown in plots D and E can be easily identified in the experimental spectra. The simulation reveals that the transmission spectrum of one iterative generation of Sierpinski Carpet structure has characteristic peaks contributed by periodic square-lattice array of apertures of 2.0 and $6.0 \mu\text{m}$, respectively. More specifically, the peaks at 161.99 and 225.63 cm^{-1} correspond to the resonance of the array of apertures of $6.0 \mu\text{m}$. The peaks at 487.90 and 682.68 cm^{-1} correspond to the resonance of array of apertures of $2.0 \mu\text{m}$.

It can be seen in Fig. 1 that there are five different aperture sizes in our Sierpinski Carpet structure. In principle, five sets of resonance peaks corresponding to the different aperture sizes should be expected. Practically, however, due to the limitation of the wave band of our spectrometers, some peaks are beyond the midinfrared and far-infrared regions and cannot be excited and measured in our system. For example, for apertures with edges of 18 , 54 , and $162 \mu\text{m}$ [the larger holes in Fig. 1(a)], the spatial periodicity of the same type of apertures increases as the hole size is increased. The resonant peaks contributed by the larger holes could exist in terahertz region, which are out of the detection range of our spectrometers.

For the metal film perforated with aperture arrays, there exist two types of resonance, the shape resonance (localized SP resonance) and surface mode of SPP.^{29,30} For the resonant peaks shown in Fig. 2, we need to pinpoint whether these peaks come from the shape resonance of each generation of apertures or whether they are induced by the surface wave diffraction. When the incident light is normal to the metal film perforated with square lattice of apertures, the wave

number of SPP-mediated resonances can be approximately expressed as¹³

$$\nu_{\max}(i,j) = \frac{\sqrt{i^2 + j^2}}{a_0 n_{\text{eff}}}, \quad (1)$$

where i and j are integers, a_0 is the lattice parameter, and n_{eff} is the real part of the effective refractive index of the perforated film. The resonance mode can be indexed as (i, j) . In our simulation (plot C in Fig. 2), five peaks are located at 161.33, 227.73, 324.22, 359.38, and 457.03 cm^{-1} . Normalizing the location of these five peaks by the lowest resonant peak at 161.33 cm^{-1} , we may find that each peak can be scaled to 1, 1.41($\sqrt{2}$), 2, 2.29($\sqrt{5}$), 2.83($\sqrt{8}$), respectively. It follows that these five peaks can be indexed as (1, 0), (1, 1), (2, 0), (2, 1), and (2, 2) according to Eq. (1). Therefore we suggest that these resonant peaks are indeed contributed by SPP-mediated surface wave diffraction on a square lattice.

Our results shown here demonstrate that with iterative generations of square apertures, extraordinary transmission can be achieved at certain wavelengths. Further, a fractal pattern, such as Sierpinski Carpet, contains hierarchy arrangement of certain geometrical unit on different scales. These units can be squeezed in a very limited geometrical space. Therefore it is possible to achieve enhanced transmission at various wavelengths simultaneously with the same integrated fractal sample. These two features imply important applications of this unique structure in miniaturization and integration of optical circuits based on SPPs, and in designing light-emitting devices, spectroscopic devices, and sensors for chemical and biological applications as well.

The authors acknowledge the financial supports from the Ministry of Science and Technology of China (2004CB619005 and 2006CB921804) and the National Science Foundation of China (10625417).

¹H. Raether, *Surface Plasmon on Smooth and Rough Surfaces and on Gratings* (Springer, Berlin, 1988).

²W. L. Barnes, A. Dereux, and T. W. Ebbesen, *Nature (London)* **424**, 824 (2003).

³S. I. Bozhevolnyi, V. S. Volkov, E. Devaux, J. Y. Laluet, and T. W.

Ebbesen, *Nature (London)* **440**, 508 (2006).

⁴S. A. Maier, P. G. Kik, H. A. Atwater, S. Meltzer, E. Harel, B. E. Koel, and A. A. G. Requicha, *Nat. Mater.* **2**, 229 (2003).

⁵J. C. Weeber, J. R. Krenn, A. Dereux, B. Lamprecht, Y. Lacroute, and J. P. Goudonnet, *Phys. Rev. B* **64**, 045411 (2001).

⁶E. Altewischer, M. P. van Exter, and J. P. Woerdman, *Nature (London)* **418**, 304 (2002).

⁷Z. W. Liu, Q. H. Wei, and X. Zhang, *Nano Lett.* **5**, 957 (2005).

⁸N. Fang, H. Lee, C. Sun, and X. Zhang, *Science* **308**, 534 (2005).

⁹H. T. Jiang, H. Chen, H. Q. Li, Y. W. Zhang, and J. Zi, *Phys. Rev. E* **69**, 066607 (2004).

¹⁰P. Andrew and W. L. Barnes, *Science* **306**, 1002 (2004).

¹¹S. I. Bozhevolnyi, V. S. Volkov, E. Devaux, and T. W. Ebbesen, *Phys. Rev. Lett.* **95**, 046802 (2005).

¹²T. W. Ebbesen, H. J. Lezec, H. F. Ghaemi, T. Thio, and P. A. Wolff, *Nature (London)* **391**, 667 (1998).

¹³H. F. Ghaemi, T. Thio, D. E. Grupp, T. W. Ebbesen, and H. J. Lezec, *Phys. Rev. B* **58**, 6779 (1998).

¹⁴A. Krishnan, T. Thio, T. J. Kima, H. J. Lezec, T. W. Ebbesen, P. A. Wolff, J. Pendry, L. Martin-Moreno, and F. J. Garcia-Vidal, *Opt. Commun.* **200**, 1 (2001).

¹⁵L. Martin-Moreno, F. J. Garcia-Vidal, H. J. Lezec, K. M. Pellerin, T. Thio, J. B. Pendry, and T. W. Ebbesen, *Phys. Rev. Lett.* **86**, 1114 (2001).

¹⁶D. X. Qu, D. Grischkowsky, and W. L. Zhang, *Opt. Lett.* **29**, 896 (2004).

¹⁷Z. C. Ruan and M. Qiu, *Phys. Rev. Lett.* **96**, 233901 (2006).

¹⁸H. A. Bethe, *Phys. Rev.* **66**, 163 (1944).

¹⁹K. J. K. Koerkamp, S. Enoch, F. B. Segerink, N. F. van Hulst, and L. Kuipers, *Phys. Rev. Lett.* **92**, 183901 (2004).

²⁰J. H. Kim and P. J. Moyer, *Opt. Express* **14**, 6595 (2006).

²¹W. J. Fan, S. Zhang, B. Minhas, K. J. Malloy, and S. R. J. Brueck, *Phys. Rev. Lett.* **94**, 033902 (2005).

²²J. R. DiMaio and J. Ballato, *Opt. Express* **14**, 2380 (2006).

²³T. Matsui, A. Agrawal, A. Nahata, and Z. V. Vardeny, *Nature (London)* **446**, 517 (2007).

²⁴J. P. Gianvittorio, J. Romeu, S. Blanch, and Y. Rahmat-Samii, *IEEE Trans. Antennas Propag.* **51**, 3088 (2003).

²⁵W. J. Wen, Z. Yang, G. Xu, Y. H. Chen, L. Zhou, W. K. Ge, C. T. Chan, and P. Sheng, *Appl. Phys. Lett.* **83**, 2106 (2003).

²⁶W. J. Wen, L. Zhou, B. Hou, C. T. Chan, and P. Sheng, *Phys. Rev. B* **72**, 153406 (2005).

²⁷S. M. Williams, A. D. Stafford, T. M. Rogers, S. R. Bishop, and J. V. Coe, *Appl. Phys. Lett.* **85**, 1472 (2004).

²⁸A. D. Rakic, A. B. Djurisic, J. M. Elazar, and M. L. Majewski, *Appl. Opt.* **37**, 5271 (1998).

²⁹C. Genet and T. W. Ebbesen, *Nature (London)* **445**, 39 (2007).

³⁰B. A. Munk, *Frequency Selective Surface, Theory and Design* (Wiley, New York, 2000).